Electron-Stimulated Reactions at the Interfaces of Amorphous Solid Water Films Driven by Long-Range Energy Transfer from the Bulk

Nikolay G. Petrik and Greg A. Kimmel*

Environmental Molecular Sciences Laboratory, Pacific Northwest National Laboratory, Mail Stop K8-88, P.O. Box 999, Richland, Washington 99352

(Received 15 October 2002; published 25 April 2003)

The electron-stimulated production of D_2 from amorphous solid D_2O deposited on Pt(111) is investigated as a function of film thickness. The D_2 yield has two components that have distinct reaction kinetics. Using isotopically layered films of H_2O and D_2O demonstrates that the D_2 is produced in reactions that occur at both the Pt/amorphous solid water (ASW) interface and the ASW/vacuum interface, but not in the bulk. The *energy* for the reactions, however, is absorbed in the bulk of the films and electronic excitations diffuse to the interfaces where they drive the reactions.

DOI: 10.1103/PhysRevLett.90.166102 PACS numbers: 82.65.+r, 34.80.Ht, 34.80.Gs, 79.20.La

The fundamental mechanisms of radiation damage to molecules in the condensed phase are of considerable interest to fields ranging from radiation biology to astrophysics. In particular, the structure of condensed water [1,2] and its interactions with electrons [3–6], photons [7], and ions [8] have been extensively studied. As a result, a variety of mechanisms for the nonthermal dissociation of water have been identified. However, the dynamics and kinetics of electronic excitations in water and their connection to the radiolysis products of water are still largely unknown.

In this Letter, we investigate the electron-stimulated production of molecular hydrogen from thin films of amorphous solid water (ASW) grown on Pt(111) as a function of film thickness. We show that there are two sources of hydrogen with distinct reaction kinetics. Experiments with isotopically layered films of D_2O and H_2O show that D_2 is produced almost entirely at the two interfaces of the films, i.e., at the ASW/Pt interface and at the ASW/vacuum interface. However, the energy that drives these reactions is absorbed within the bulk of the film. The results suggest that electronic excitations in the bulk of the film diffuse to either interface prior to reacting and that electron-stimulated reactions are significantly enhanced at interfaces as compared to the bulk.

The experiments were performed in an ultrahigh vacuum system equipped with an electron gun, two effusive gas dosers, and a quadrupole mass spectrometer. Dense, relatively smooth ASW films with surface areas that are approximately independent of film thickness were grown on Pt(111) at 100 K [2]. The Pt(111) sample was cleaned by annealing in oxygen, followed by argon ion sputtering and annealing in vacuum. For temperature programmed desorption (TPD) of water on Pt(111), the monolayer (ML) peak shape is very sensitive to contamination and this was used to monitor the sample cleanliness [9]. The area of the saturated ML peak in TPD ($\equiv 1$ ML) was used to calibrate the coverage, θ, with an estimated uncertainty of $\pm 15\%$. The ASW films were irradiated at 100 K, with 100 eV electrons in 240 s beam pulses, at 45° angle of incidence, with typical current densities of $\sim 6 \times 10^{13}$ electrons/cm^2 s and beam spot sizes of ~ 1.5 mm. For these conditions, sputtering of the ASW film by the electron beam results in less than 1 ML change in coverage.

The electron-stimulated desorption (ESD) yield of D_2 as a function of time for two D_2O films is shown in Fig. 1. The D_2 yield from a 20 ML D_2O film [Fig. 1(a)] demonstrates two features common to thin films. First, the D_2 yield promptly increases at the beginning of the electron pulse. Second, this prompt component is followed by a slowly increasing, dose-dependent component that eventually saturates. In contrast to the thinner film, the D_2 yield from the 120 ML ASW film [Fig. 1(b)] is approximately constant. Another noticeable difference between "thin" (20 ML) and "thick" (120 ML) ASW films is the evolution of D_2 after the electron beam has been turned

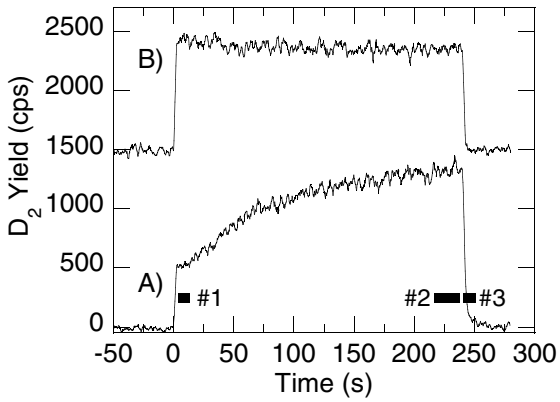

FIG. 1. Electron-stimulated D_2 yield from D_2O ASW films adsorbed on Pt(111) vs time. The curves are displaced for clarity. Curve *A* (*B*) shows the D_2 yield from a 20 (120) ML film of D_2O. The bars on curve *A* schematically indicate the time intervals for calculating the prompt (No. 1), total (No. 2), and postirradiation (No. 3) integrated D_2 yields in Figs. 2 and 3.

 © 2003 The American Physical Society

off. For thicker films, the decrease in the D_2 yield is relatively abrupt at the end of the pulse compared to thinner films. The data shown in Fig. 1 suggest that there are two distinct components, with different reaction kinetics, contributing to the ESD yield.

Figure 2 shows the D_2 ESD yield as a function of ASW film thickness for $0 \leq \theta < 200$ ML. To assess the thickness dependence of the prompt D_2, we measure the D_2 yield during the first 2 s of the irradiation [interval No. 1 in Fig. 1(a)]. The total D_2 yield is measured during the last 10 s of the irradiation [interval No. 2 in Fig. 1(a)]. Assuming that the prompt D_2 yield is constant, the dose-dependent D_2 yield is then given by the difference between the total and the prompt D_2 yields. We have also measured the postirradiation D_2 that desorbs from the film in a 1 s window that starts 1 s after the end of the electron pulse [interval No. 3 in Fig. 1(a)]. The total D_2 yield has a maximum at $\theta \sim 25$ ML and decreases to a coverage independent value for $\theta > 100$ ML [Fig. 2(a)]. The prompt D_2 increases monotonically for $\theta < 100$ ML and is constant for higher coverages [Fig. 2(a)]. The dose-dependent and postirradiation D_2 yields are similar, both going through a maximum at $\theta \sim 25$ ML and declining to approximately zero for $\theta > 100$ ML [Fig. 2(b)]. Note that the thickness over which the D_2 yield is changing is $\sim$100 ML, suggesting that energy deposited into the film contributes to the D_2 ESD yield over that length scale.

To investigate where in the films the D_2 is produced, we have used isotopically layered films of D_2O and H_2O. The D_2 ESD yield versus time for a 26 ML film of pure D_2O [Fig. 3(a), curve 1] has the characteristic shape discussed above [Fig. 1(a)]. However, when a 20 ML D_2O film is capped with a 6 ML H_2O film [Fig. 3(a), curve 2], the prompt D_2 yield is suppressed while the dose-dependent D_2 yield is essentially unchanged. Conversely, when a 6 ML H_2O spacer layer is deposited on the Pt(111) first followed by a 19 ML film of D_2O, the dose-dependent D_2 yield is suppressed while the prompt D_2 is essentially unchanged [Fig. 3(a), curve 3].

Figure 3(b) shows the prompt D_2 yields (solid circles, calculated using the procedure described for Fig. 2) for a 20 ML D_2O film versus the coverage of the H_2O capping layer. The prompt D_2 yield decreases approximately exponentially with increasing H_2O coverage with a $1/e$ constant of $\sim 2.3 \pm 0.3$ ML. (The dose-dependent D_2 yield decreases slightly due to the increasing total thickness of the ASW film; data not shown.) Experiments with H_2O capping layers on thicker D_2O films (100 to 400 ML) gave similar results for the prompt D_2 yield with a similar decay constant. Therefore, surface

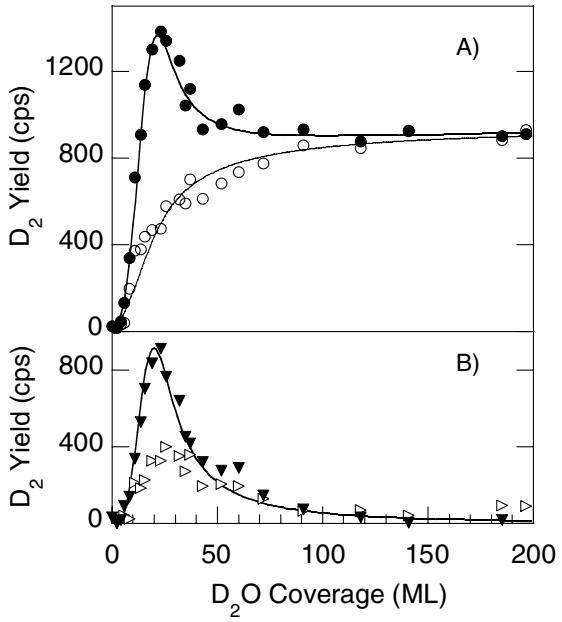

FIG. 2. Electron-stimulated D_2 yields vs ASW film thickness. (A) Prompt D_2 (open circles) and total D_2 yields (solid circles). (B) Dose-dependent D_2 (solid triangles) and postirradiation D_2 yields (open triangles). The lines are the results of a model fit to the data (see text).

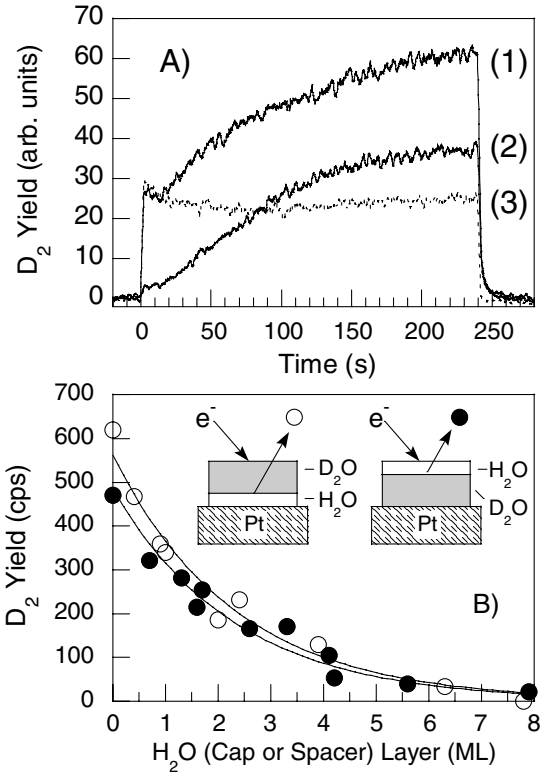

FIG. 3. (A) Electron-stimulated D_2 yield vs time from a pure 26 ML D_2O film (curve 1), from an isotopically layered ASW film of 20 ML D_2O film capped with 6 ML of H_2O (curve 2), and a 19 ML D_2O film on top of 6 ML of H_2O (curve 3). (B) Prompt D_2 (solid circles) yield vs the thickness of an H_2O layer deposited on the top of a 20 ML D_2O film and dose-dependent D_2 (open circles) yield vs the thickness of an H_2O film deposited underneath a 25 ML D_2O film. The solid lines are exponential fits to the data.

roughness is probably not primarily responsible for the observed decay length. Figure 3(b) also shows the dose-dependent D_2 yields (open circles) for a 25 ML D_2O film versus the H_2O spacer layer coverage on the Pt(111). The dose-dependent D_2 also decays exponentially with a $1/e$ constant of $\sim 2.3 \pm 0.3$ ML. (The prompt yield increases slightly due to the increasing total thickness of the ASW film; data not shown.) In the experiments with the H_2O capping and spacer layers, we also observed a small HD signal associated with the H_2O/D_2O interface *which was independent of the* H_2O *thickness for* H_2O *coverages greater than* ~ 0.5 ML.

The data in Fig. 3 show that: (1) D_2 produced in D_2O readily diffuses out at 100 K. (2) The isotope exchange reaction, $D_2 + H_2O \rightarrow HD + HDO$, is not important here. (3) The prompt D_2 is produced within the first several monolayers of the ASW film near the vacuum interface, while the dose-dependent D_2 originates in the ASW film within a few monolayers of the Pt substrate. (4) The postirradiation D_2 results from D_2 produced at the Pt/ASW interface that subsequently diffuses out. Thus, for these experiments, *essentially all the electron-stimulated reactions producing* D_2 *occur at the inner and outer interfaces of the* D_2O *film*. Within the sensitivity of the experiments, no D_2 is produced in the bulk of the ASW. On the other hand, *the energy for the reactions is primarily absorbed in the bulk of the film* and therefore must be transported to the interfaces over lengths of ~ 100 ML. There are several mechanisms by which the energy that is absorbed in the bulk might reach the interfaces, including the diffusion of atomic or molecular precursors and the diffusion of electronic excitations.

The D_2 ESD at the ASW/vacuum interface probably results from unimolecular decay of D_2O^* or D_3O^* resulting from electron-ion recombination and direct excitation [10,11]. The kinetics observed for the reaction are consistent with this picture: The yield of D_2 from the ASW/vacuum interface is proportional to the incident electron flux and approximately independent of the electron fluence. Calculations show that ionization is the dominant energy loss mechanism for 100 eV electrons in water [12], and the D_2 yield as a function of electron energy [5,13] suggests that at 100 eV ionization is the initial step in the reactions leading to D_2. While dissociative electron attachment (DEA) reactions contribute to the D_2 yield [5], they are probably not a major component of the reactions at the vacuum interface since the D_2 yield per electron at 100 eV is much greater than the D_2 yield in the range where DEA is important (~ 10 eV). Ionization followed by electron-ion recombination and unimolecular decay of excited neutral molecules has also been implicated in the ESD of D and O atoms from ASW [4].

The kinetics of the reactions at the Pt/ASW interface are more complex than those at the ASW/vacuum interface. For ASW films of constant thickness, we have measured the D_2 yield as a function of time for a variety of incident electron currents. When that data is plotted as the dose-dependent D_2 yield divided by the electron beam flux versus the electron fluence (i.e., dose time $\times$ electron flux), the data fall on a universal curve. This result suggests that the dose-dependent D_2 ESD involves the creation of a precursor followed by a second reaction leading to D_2. If a previously irradiated sample is reirradiated, the D_2 yield promptly returns to the level obtained at the end of the prior irradiation, suggesting that the precursor species is relatively stable (for at least 1 h). Qualitatively similar behavior was observed for O_2 produced by electron irradiation of ASW [14]. In that case, an HO_2 or H_2O_2 precursor was implicated.

The data argue against the species that is made in the bulk of the film and transported to the interfaces being atomic or molecular. First, in the isotopic labeling experiments, very little HD is produced as would be expected if D atoms or any deuterium-containing molecule produced in the bulk were involved in the reactions at the interface. Second, the D ESD yield versus thickness (data not shown) is different than that of D_2. Third, earlier ESD experiments that investigated the velocity distributions of D [6], O, and D_2 [15] and the rotational state distributions of D_2 [10] as a function of temperature found evidence for the rapid diffusion of energy, but not atoms or molecules, from the bulk of the film to the ASW/vacuum interface. Therefore, it is likely that some form of electronic excitation is responsible for transporting the energy deposited in the bulk to the interfaces where it reacts to form D_2.

There is very little information on the dynamics of low-energy electronic excitations in ASW. However, delocalized electrons [16], holes [17], and excitons [6,18] in condensed water have all been proposed. Ionization in the bulk of the film is rapidly followed by either electron-ion recombination or the formation of hydronium, H_3O^+ [19]. However, recent experiments showing that hydronium ions have very limited mobility in ASW at 100 K argue against these being responsible for transporting the energy from the bulk to the interfaces [20]. Furthermore, if the hydronium ions are immobile, then the electron-ion recombination should also occur predominantly in the bulk of the film. Therefore, excitons are probably responsible for transferring energy from the bulk to the interfaces.

The results in Fig. 2 can be qualitatively reproduced with a simple model that treats diffusion of an excitation from the bulk of the film to either interface. In a random walk, the probability of an excitation, created at x, in a film of thickness L, reaching either interface is given by $P_{\mathrm{vac}}(x) = 1 - x/L$ and $P_{\mathrm{Pt}}(x) = x/L$, where P_{vac} and P_{Pt} are the probability of an excitation reaching the ASW/vacuum or Pt/ASW interface, respectively. (The ASW/vacuum interface is defined to be at $x = 0$.) The total flux reaching either interface from excitations created throughout the film is $\Phi_i = \int_0^L P_i(x) n_{\mathrm{ex}}(x) dx$, where

$n_{ex}(x)$ is the number of excitations per unit length created by the electron beam and i = Pt or vac for reactions at the Pt or vacuum interfaces, respectively. Calculations of the energy loss, dE/dx, of an electron in water [21] suggest that it is approximately Gaussian for $0 \leq x \leq L$, $dE/dx(x) = \exp[-(x - x_0)^2/\sigma^2]$ and we assume that n_{ex} is proportional to dE/dx [22]. As discussed above, the prompt D_2 yield, Y_{vac}, is proportional to the total excitation flux reflecting the first order kinetics of that reaction: $Y_{vac} \sim \Phi_{vac}$. The dose-dependent D_2 yield, Y_{Pt}, is proportional to the square of the total excitation flux due to the second order reaction kinetics: $Y_{Pt} \sim (\Phi_{Pt})^2$.

The solid lines in Fig. 2 show the model fit to the data with $x_0 = 10$ ML and $\sigma = 10$ ML. In this model, the maximum in the total yield arises when the film is sufficiently thick to absorb most of the energy from the incident beam, but thin enough that the excitations are still likely to reach the Pt/ASW interface (which is assumed to have a higher reaction probability). For thicker films, the total D_2 yield decreases since the flux of excitations reaching the Pt/ASW interface is lower. For $\theta >$ 25 ML, the prompt D_2 yield [Fig. 2(a)] is proportional to $1 - C/L$ while the dose-dependent D_2 yield [Fig. 2(b)] is proportional to $1/L^2$. This is the expected result from the model: For $L > L_e$, we have $\Phi_{Pt} \sim C/L$ and $\Phi_{vac} \sim 1 - C/L$, where L_e characterizes the maximum penetration of the incident electrons into the ASW and $C = \int_0^{L_e} x n_{ex}(x) dx$ = const. In general, this simplified model captures the basic features of the D_2 ESD yield versus D_2O thickness.

The diffusion of excitons to the surface plays an important role in electron- and photon-stimulated desorption in alkali halides [23] and is similar to the mechanism proposed here for ASW. The apparently low probability for these excitations to dissociate in the bulk leading to molecular hydrogen is noteworthy. The lack of D_2 formation in the bulk may be due to "cage" effects, where the surrounding molecules prevent the dissociation of electronically excited water molecules. Alternatively, the diffusion time for the excitation may be fast compared to the dissociation time scale, suppressing dissociation. The changes in both the geometrical and the electronic structure of the water molecules at the ASW/vacuum interface are likely to favor reactions there. First, the cage effect should disappear. Second, the partially coordinated molecules at the vacuum interface may lead to localization of the excitation. At the Pt/ASW interface, the perturbation of the water bonding structure [24] may facilitate the reactions leading to the precursor molecule and the dose-dependent D_2.

In summary, we find that the low-energy, electron-stimulated production of molecular hydrogen in ASW occurs only at the interfaces of the ASW film. However, the energy that drives these reactions is deposited in the bulk of the film, and the diffusion of electronic excitations subsequently carries the energy to the interfaces.

This work was supported by the U.S. Department of Energy, Office of Basic Energy Sciences, Chemical Sciences Division. Pacific Northwest National Laboratory is operated for the U.S. Department of Energy by Battelle Memorial Institute under Contract No. DE-AC06-76RLO 1830.

*Corresponding author.
Email address: gregory.kimmel@pnl.gov

[1] E. Mayer and R. Pletzer, Nature (London) **319**, 298 (1986); J.-H. Guo *et al.*, Phys. Rev. Lett. **89**, 137402 (2002).
[2] K. P. Stevenson *et al.*, Science **283**, 1505 (1999); G. A. Kimmel *et al.*, J. Chem. Phys. **114**, 5284 (2000).
[3] P. Rowntree, L. Parenteau, and L. Sanche, J. Chem. Phys. **95**, 8570 (1991); J. O. Noell, C. F. Melius, and R. H. Stulen, Surf. Sci. **157**, 119 (1985).
[4] G. A. Kimmel and T. M. Orlando, Phys. Rev. Lett. **75**, 2606 (1995).
[5] G. A. Kimmel and T. M. Orlando, Phys. Rev. Lett. **77**, 3983 (1996).
[6] T. M. Orlando and G. A. Kimmel, Surf. Sci. **390**, 79 (1997).
[7] M. S. Westley *et al.*, Nature (London) **373**, 405 (1995).
[8] W. L. Brown, L. J. Lanzerotti, and R. E. Johnson, Science **218**, 525 (1982).
[9] J. L. Daschbach and B. D. Kay (private communication).
[10] G. A. Kimmel, R. G. Tonkyn, and T. M. Orlando, Nucl. Instrum. Methods Phys. Res., Sect. B **101**, 179 (1995).
[11] B. R. Rowe *et al.*, J. Chem. Phys. **88**, 845 (1988); N. G. Adams *et al.*, J. Chem. Phys. **94**, 4852 (1991).
[12] S. M. Pimblott and A. Mozumder, J. Phys. Chem. **95**, 7291 (1991).
[13] G. A. Kimmel *et al.*, J. Chem. Phys. **101**, 3282 (1994).
[14] M. T. Sieger, W. C. Simpson, and T. M. Orlando, Nature (London) **394**, 554 (1998).
[15] G. A. Kimmel and T. M. Orlando (unpublished).
[16] A. Bernas, C. Ferradini, and J. P. Jay-Gerin, Chem. Phys. **222**, 151 (1997).
[17] R. Souda, J. Phys. Chem. B **105**, 5 (2001).
[18] K. Kobayashi, J. Phys. Chem. **87**, 4317 (1983); V. Y. Sukhonosov, High Energy Chem. **32**, 71 (1998).
[19] M. Kunst and J. M. Warman, J. Phys. Chem. **87**, 4093 (1983).
[20] J. P. Cowin *et al.*, Nature (London) **398**, 405 (1999).
[21] J. A. Laverne and S. M. Pimblott, J. Phys. Chem. A **101**, 4504 (1997).
[22] If the excitons are formed by electron-ion recombination after ionization, then we might expect $n_{ex}(x)$ to be proportional to the square of the number of ionizations, $n_{ion}(x)$, per unit length, which is also Gaussian.
[23] See, for example, K. S. Song and R. T. Williams, *Self-Trapped Excitons* (Springer, Berlin, 1996), 2nd ed., and references therein.
[24] H. Ogasawara *et al.*, Phys. Rev. Lett. **89**, 276102 (2002).